Microinstabilities in the Confinement Zone near the Tokamak Edge

C M Roach[1], P Abdoul[2], M Anastopoulos[2] J W Connor[1], D Dickinson[2], R J Hastie[1], S Saarelma[1], and H R Wilson[2]

[1] *CCFE, Culham Science Centre, Abingdon, OX14 3DB, UK*

[2] *York Plasma Inst., Dep't of Physics, University of York, Heslington, York, YO10 5DD, UK*

Introduction

Microturbulence influences transport in the edge region of tokamak H-mode plasmas, and the pedestal characteristics that are crucial for overall plasma performance. Local gyrokinetic calculations for MAST [1, 2] find that, at perpendicular lengthscales close to ρ_i, electromagnetic microinstabilities dominate with a striking mode transition at the pedestal top: microtearing modes (MTMs) dominate in the plateau inboard of the pedestal top, while twisting parity kinetic ballooning modes (KBMs) dominate in the pedestal itself. This paper reviews recent findings on: mode transitions at the MAST pedestal top, physics impacting on the (marginal) stability of KBMs in the pedestal, and microtearing modes in the plateau.

Mode Transitions at the Pedestal Top: ETG also unstable in Plateau

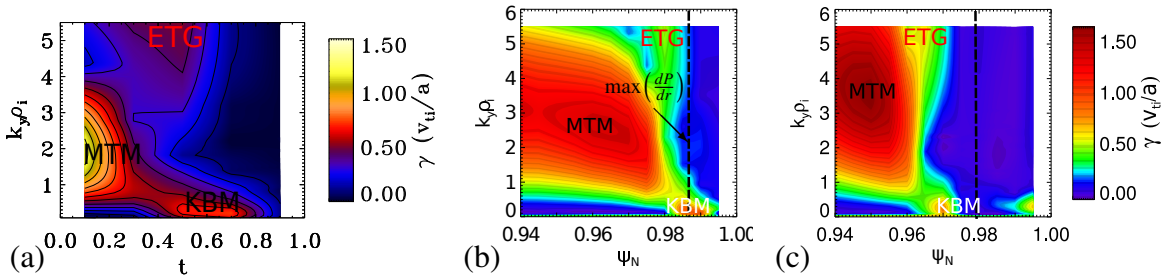

Figure 1: *(a) $\gamma(k_y\rho_i, t)$ of the dominant mode at the $\psi_n = 0.975$ surface (where t is normalised time during the ELM recovery). (b), (c) $\gamma(k_y\rho_i, \psi_n)$ at the start and end of the ELM recovery, respectively.*

As the MAST pedestal expands inwards during the ELM recovery [3], dn_e/dr and dP/dr increase on a plateau plasma surface as it joins the pedestal, which acts to stabilise MTMs until the onset of KBMs at higher dP/dr [1]. Subsequent studies reveal that ETG is *also unstable* at higher $k_y\rho_i$ in the MAST plateau, and *also stabilised* as dn_e/dr increases on a plateau surface joining the pedestal. Figure 1 shows that microstability spectra from [1, 2] *contain the low $k_y\rho_i$ tail of the ETG peak*. DBS and CPS measurements of δn and δB fluctuations at the MAST pedestal top during ELM recovery, appear consistent with linear ETG properties from GS2 [4].

Impact of ν_* and Global Effects on KBMs in the Pedestal

KBMs are locally unstable, but close to marginal [1], in most of the collisional MAST pedestal studied in [1], but in lower ν_* MAST pedestals KBMs are locally stable across most of the

[1] ASDEX Upgrade pedestals are also close to the KBM limit [5].

steep gradient region [2], as has also been found for JET pedestals [6]. This increased stability at lower ν_* is due to higher bootstrap current density, J_{bs}, reducing magnetic shear, s, and improving access to 2nd stability. The sensitivity of the absolute local stability of KBMs to J_{bs} will motivate the future use of more accurate bootstrap current models, e.g. [7].

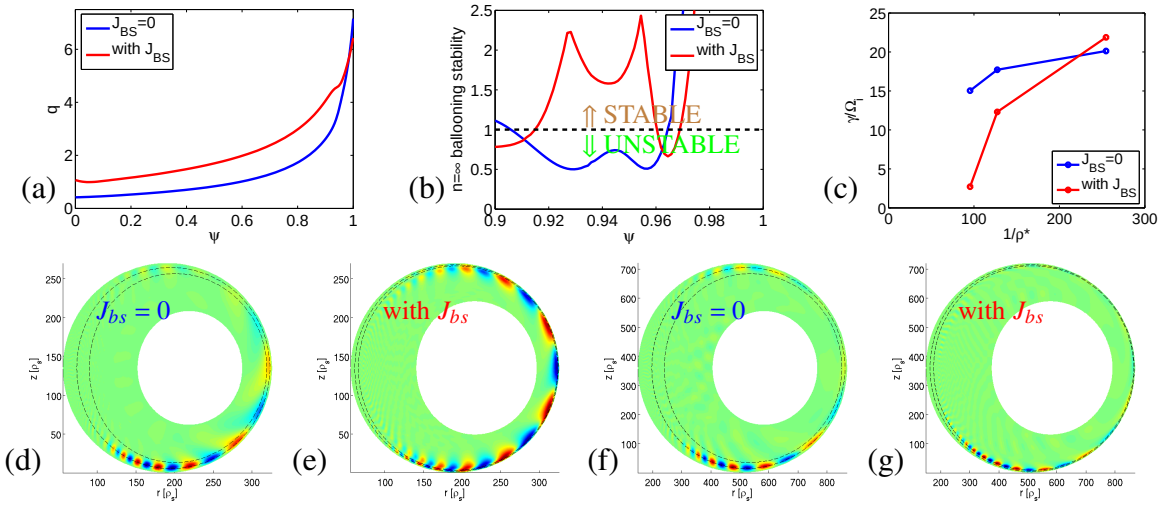

Figure 2: *(a) q profiles and (b) ideal $n = \infty$ ballooning stability index from circular MAST-like equilibria with/without J_{bs}. (c) Corresponding growth rates of $n = 10$ KBM, from ORB5, as functions of $1/\rho_*$. Eigenfunctions of electrostatic potential with,without J_{bs} (d),(e) for $1/\rho_* = 95$, and (f),(g) for $1/\rho_* = 254$.*

Global effects are also significant for ion scale instabilities in the pedestal as $\rho_i/L \not\ll 1$. Global mode properties can be determined by post-processing results from local gyrokinetic calculations (see [8, 9]). This reveals that global profile effects impact on the linear eigenmodes and reduce growth rates below those obtained from purely local analyses, as demonstrated for ITG in [9]. In future we will compare the local post-processing approach of [9] with linear global GK calculations of KBMs in the pedestal (using ORB5). Two circular MAST-like equilibria were generated with and without J_{bs}, with the q profiles given in Figure 2(a). Figure 2(b) shows $n = \infty$ ballooning stability index profiles, indicating that the ballooning unstable region of the pedestal narrows with J_{bs}. Figure 2(c) shows linear growth rates for the $n = 10$ KBM from global GK calculations using ORB5 over a scan in $1/\rho_*$, and figures 2(d-g) show electrostatic potential eigenfunctions. At low $1/\rho_*$, where global effects are stronger, the KBM is more extended radially and less unstable. The global effects are more strongly stabilising in the case with J_{bs} included, because the mode must extend into a locally stable region.

Studies of Microtearing Modes

MTMs are unstable in the MAST plateau without collisions, and growth rates are sensitive to drifts [10]. [2] Linear collisionless local gyrokinetic calculations using GS2, GKW and GENE for

[2]MTMs with similar properties are also unstable in the JET plateau [6], and were recently found in global

a circular equilibrium surface based on MAST plateau equilibrium parameters, find dominant MTMs with similar growth rate and frequency spectra (see Figure 3).

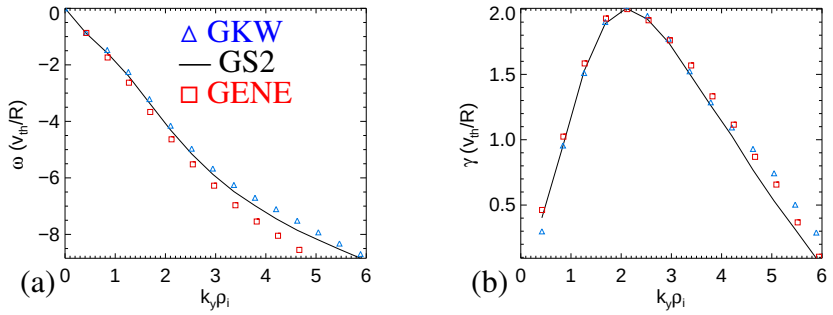

Figure 3: *(a) Real frequency, ω, and (b) growth rate, γ, of dominant MTMs versus $k_y\rho_i$ from local linear collisionless GK calculations using GS2, GKW and GENE, for a circular MAST-like plateau surface.*

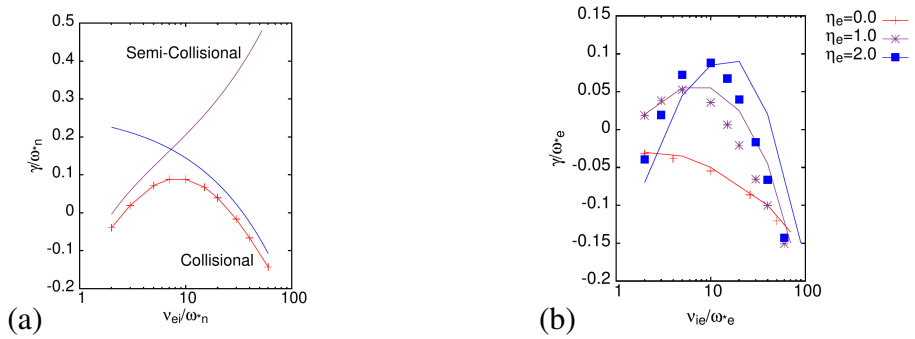

Figure 4: *MTM growth rates from GS2 versus electron collision frequency compared (a) with scalings in the collisional (blue) and semi-collisional (purple) limits obtained by Drake and Lee [12] at $\eta_e = 2$, and (b) at $\eta_e = 0, 1, 2$ with the model by Gladd* et al *[13].*

GS2 calculations of MTMs in slab geometry [14], with equilibrium parameters $\beta_e = 0.005$, $L_n/L_s = 0.05$, $k_y\rho_i = 0.05$ and various values of $\eta_e = L_{n_e}/L_{T_e}$, capture the trends predicted by theory for another microtearing instability mechanism that relies on collisions [12, 13]. Figure 4 shows MTM growth rates from GS2 versus electron collision frequency, comparing in Figure 4(a) with predictions by Drake and Lee [12], and in Figure 4(b) with calculations by Gladd *et al* [13] that more fully account for the electrostatic impact on the current layer.

Nonlinear MTM simulations at the MAST pedestal top predict significant electron heat flux, but convergence was only achieved with β a factor 5 smaller than in experiment [15]. Edge fluctuation measurements in MAST [16] and ASDEX Upgrade [17], find type-I ELM precursors that propagate in the electron diamagnetic drift direction, and may be consistent with MTMs.

Conclusions

Local gyrokinetic simulations suggest that electromagnetic microinstabilities play an important role at the edge of the confinement zone in MAST H-mode plasmas: MTMs and ETG dominate in the plateau region, and KBMs, which are sensitive to collisionality and global effects,

simulations of large aspect ratio tokamaks [11].

are close to marginal stability in the pedestal. Both ETG and MTM are stabilised as dn_e/dr increases on a plateau surface as it joins the pedestal during the ELM recovery. The plateau MTM is unstable without collisions, and its linear mode properties have been verified, for circular shaping, by three local gyrokinetic codes. GS2 captures predictions for the scaling of MTM growth rates with ν_e in slab geometry where the MTM drive requires collisions. Nonlinear simulations are needed for more realistic plasma conditions in the edge plasma, to improve contact with edge fluctuation measurements.

Acknowledgements

This work has been carried out within the framework of the EUROfusion Consortium and has received funding from the Euratom research and training programme 2014-2018 under grant agreement No 633053 and from the RCUK Energy Programme [grant number EP/I501045]. The views and opinions expressed herein do not necessarily reflect those of the European Commission. GK calculations were carried out on supercomputers: HELIOS at IFERC, Aomori, Japan under the Broader Approach; ARCHER via the Plasma HEC Consortium [EPSRC Grant No.EP/L000237/1]; and HECToR [EPSRC Grant No. EP/H002081/1]. The authors are grateful for useful discussions with FJ Casson, H Doerk, J Hillesheim, A Kirk, R Scannell and D Told.

References

[1] D. Dickinson et al., Physical Review Letters **108**, 135002 (2012). **[2]** C. M. Roach et al., in Proceedings of 24th IAEA Fusion Energy Conference, San Diego, pp. (TH/5–1), 2012. **[3]** D. Dickinson et al., Plasma Phys. Controlled Fusion **53**, 115010 (2011). **[4]** J. C. Hillesheim et al., submitted to Plasma Phys. Controlled Fusion (2015). **[5]** D. Hatch et al., Nuclear Fusion **55**, 063028 (2015). **[6]** S. Saarelma et al., Nuclear Fusion **53**, 123012 (2013). **[7]** E. A. Belli et al., Plasma Phys. Controlled Fusion **56**, 045006 (2014). **[8]** D. Dickinson et al., Physics of Plasmas **21**, 010702 (2014). **[9]** P. A. Abdoul et al., Plasma Phys. Controlled Fusion **57**, 065004 (2015). **[10]** D. Dickinson et al., Plasma Phys. Controlled Fusion **55**, 074006 (2013). **[11]** A. K. Swamy et al., Physics of Plasmas **21**, 082513 (2014). **[12]** J. F. Drake and Y. C. Lee, Phys Fluids **20**, 1341 (1977). **[13]** N. T. Gladd et al., Phys Fluids **23**, 1182 (1980). **[14]** M. Anastopoulos, Mphys project dissertation, University of York, 2015. **[15]** D. Dickinson et al., in Proceedings of 40th EPS Conference on Plasma Physics, Strasbourg, France, Vol. ECA 37D, O3.105, 2013. **[16]** A. Kirk et al., Nuc. Fusion **54**, 114012 (2014). **[17]** P. Manz et al., Plasma Phys. Controlled Fusion **56**, 035010 (2014).